We are IntechOpen, the world's leading publisher of Open Access books Built by scientists, for scientists

4,800
Open access books available

122,000
International authors and editors

135M
Downloads

Our authors are among the

154
Countries delivered to

TOP 1%
most cited scientists

12.2%
Contributors from top 500 universities

WEB OF SCIENCE™

Selection of our books indexed in the Book Citation Index in Web of Science™ Core Collection (BKCI)

Interested in publishing with us?
Contact book.department@intechopen.com

Numbers displayed above are based on latest data collected.
For more information visit www.intechopen.com

Chapter 26

Active Control of Plate-Like Structures for Vibration and Sound Suppression

Ipek Basdogan, Utku Boz, Serkan Kulah and Mustafa Ugur Aridogan

Additional information is available at the end of the chapter

http://dx.doi.org/10.5772/51755

1. Introduction

Mechanical vibrations cause undesirable effects such as noise and acoustic signature and consequences of severe vibrations may lead to a decrease in service life of machines, or even cause damages on the components. In order to reduce vibration levels in ground, marine and aerospace applications as well as nano and micro devices, active control methods for vibration and noise reduction has been proposed in the last decade.

In 1980s, the usages of large structures as the components of the space vehicles were resulted in new challenges in vibration control since these structures are lightly damped and have long decay times. Researchers were motivated to design and implement active vibration control to these lightly damped structures with piezoelectric materials. In one of the first research studies relevant to this area, Bailey and Hubbard [1] designed an active damper system by using piezoelectric material as distributed actuator for the vibration suppression of a cantilever beam. Subsequently, Crawley and Luis [2] developed and experimentally verified the analytical model of piezoelectric materials. The main contribution of Crawley and Luis was the accurate prediction of performance and effectiveness of piezoelectric materials when they are used as actuators. While passive isolation techniques are not generally feasible and efficient for low frequency vibration suppression; aforementioned initiative studies showed that piezoelectric materials can be used to suppress the low frequency vibration. Indeed, Ro and Baz [3] investigated and compared the overall effectiveness of the active and passive treatments for vibration and noise reduction. Their results revealed that active treatments such as bonded piezoelectric patch actuators can significantly reduce the vibration and noise radiation better than the passive treatments. Currently, different types of piezoelectric elements are available in market which can be employed widely as actuators and sensors for active vibration reduction of structures.

In the literature, there are published review articles discussing fundamental aspects of active vibration control. Rao and Sunar [4] published a review paper on the use of piezoelectric materials as sensors and actuators for control of flexible structures. In this review paper, they presented the general framework of structural control strategies and presented the applications in various fields. One of the most common application areas is aerospace industry, since the aerospace structures are flexible and have limited tolerance for vibration. In a different review study, Loewy [5] presented the key applications of smart structures in aeronautical applications with potential usages. In this work, smart materials are categorized in terms of their energy-exchange capabilities. The benefits of using smart structures in aeronautical applications are also presented.

The active vibration control systems should be feasible and reliable to be used in marine, aerospace and automotive applications. The reliability and feasibility of the control systems are related to dynamics of piezoelectric actuators and implementation of controller algorithms. Thus, it is needed to predict performance of the piezoelectric sensor and actuators embedded in control systems before implementation and production. For this purpose, Chee et al. [6] presented the modeling approaches for performance investigation of piezoelectric materials. As discussed in their article, analytical and finite element modeling of piezoelectric materials with host structures can be built using the linear constitutive piezoelectric equations only for low actuation authority. In case of high actuation authority; the nonlinearities occurs and different methodologies should be considered.

The choice of the controller type and optimal positioning of sensors and actuators are other important aspects of design and implementation of active vibration control systems. There are also published technical review papers discussing the controller algorithms and optimal placement of actuators and sensors. For instance, Alkhatib and Golnaraghi [7] reviewed the controller architectures and presented the general design procedures for the active vibration control systems. In this review paper, the advantages and disadvantages of different controller architectures with various application examples are presented. Specifically that review paper states that the active damping system is advantageous when the vibration suppression is aimed only around resonance frequencies. It is also noted that the active damping system ensures stability when collocated sensor and actuator pairs are used. In another review paper, Gupta et al. [8] concentrated on the optimal positioning of piezoelectric sensors and actuators. In this technical review, the optimization techniques are presented based upon six optimizing criteria, namely (i) maximizing modal forces/moments applied by piezoelectric actuators, (ii) maximizing deflection of the host structure, (iii) minimizing control effort/maximizing energy dissipated, (iv) maximizing degree of controllability, (v) maximizing degree of observability, and (vi) minimizing spill-over effects. Gupta et al. presented the optimal positioning results in the literature in a tabular form for beam and plate like structures.

For robust and adaptive active vibration control systems, the structural modeling techniques and estimation of uncertainties are important. A comprehensive methodology for the design

and validation of a robust controller is presented by Iorga et al. [9]. In their paper, structural modeling techniques with uncertainty analysis are explained and H_∞ controller design is pursued by placing emphasis on robust control concepts.

The piezoelectric materials also attracted attention of the researchers working on noise reduction. In a review paper on smart structures and integrated systems, Chopra [10] stated that most of the applications for aerospace vehicles are focused on minimization of vibration levels; however, interior and exterior noise reduction, using piezoelectric materials is also a potential research area for transport vehicles. Hanselka [11] named the use of smart materials in active noise and vibration control as an innovative technology and gave an application example of active noise reduction. In that application, piezoelectric materials served as sensors and actuators to reduce structural-borne noise and the results showed that the application of current developments is possible and advantageous.

This chapter is organized as follows. In section 2, the design procedure and algorithms for active vibration and noise control systems are explained briefly. In section 3, a proportional velocity feedback implementation for active vibration control system developed in our laboratory is presented. Finally, the vibration and noise reduction performance of the controller is discussed.

2. Active vibration and noise control system design

2.1. Design procedure

Undesired mechanical vibrations and noise can be avoided or minimized by active vibration and noise control systems. The design of such systems starts with the dynamic characterization of the target structure that is called host structure for embedding or bonding the smart materials. The dynamic characterization procedure can be carried out numerically and/or experimentally by investigating the vibration characteristics of the structure. By utilizing sensors and actuators, system identification methods can be applied for modeling the whole system. The next step is the reduction of the developed model such that the computations can be performed in a reasonable time. In fact, the model reduction techniques shall be applied while considering the controllability and observability properties of the system. The steps between the characterization of the host structure and the reduced order model are referred as “modeling stage”. Having determined the reduced-order model, the controller is designed and configured until the performance objectives are met. This stage is called the controller stage where the aim is to design and implement the controller for the performance requirements. The design steps of modeling and controller stages are presented in flow chart by Preumont [12] and depicted in Fig. 1. In the next section, the controller architectures will be discussed in detail.

2.2. Selection of controller architecture

This section presents an overview of controller algorithms for active vibration and noise control systems. In general, the controllers are designed for two different tasks: tracking a

trajectory or rejecting disturbances. For active vibration suppression systems, the task is the rejection of external disturbances and reduction of vibration levels. These can be achieved via feedback and feedforward controllers. The generic block diagrams [7] of these controller algorithms are presented in Fig. 2a and Fig. 2b. Basically, the feedback controller generates controller output signal based on summation of plant response and external disturbance. On the other hand, feedforward controller generates controller output by measuring external disturbance and predicting the plant response.

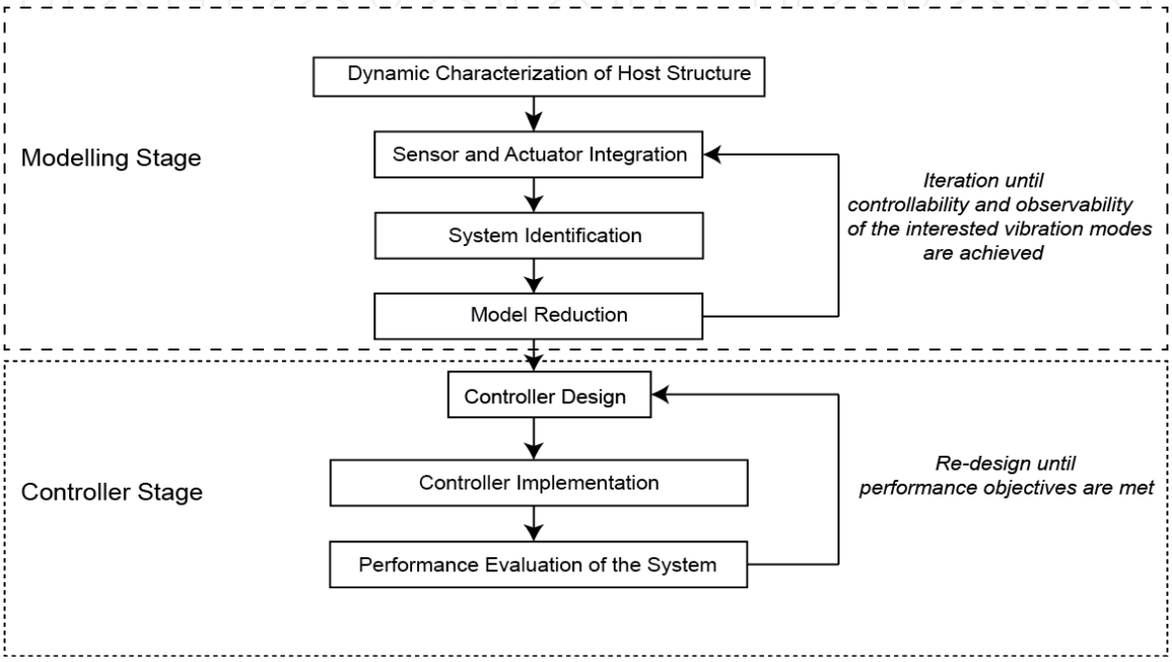

Figure 1. Control System Design Steps

The feedback controller algorithms can be divided into two categories [13] : active damping systems and model-based controllers. In an active damping system, the vibration of the host structure (acceleration, velocity or displacement) can be suppressed around the resonance frequencies. The closed-loop transfer function of the active damping system can be derived by using the block diagram shown in Fig. 2a as it follows:

$$y = d + uG(s) \tag{1}$$

Here, the sensor output signal is denoted by y, external disturbance is shown with d and controller output is u. The open-loop system is presented with G(s) in Laplace domain. After algebraic manipulations, one can obtain the following relation for the closed-loop system:

$$y = \frac{1}{1+C(s)G(s)}d \tag{2}$$

In Equation 2, the closed-loop transfer function shows that the effect of external disturbance on the sensor output can be minimized by increasing the magnitude of the $C(s)G(s)$ as the phase and gain margin of the open-loop system $G(s)$ allows. Since the collocated sensor and actuator pair provides infinite gain and phase margins, the active damping system works very efficiently when the collocated sensor and actuator pair is used.

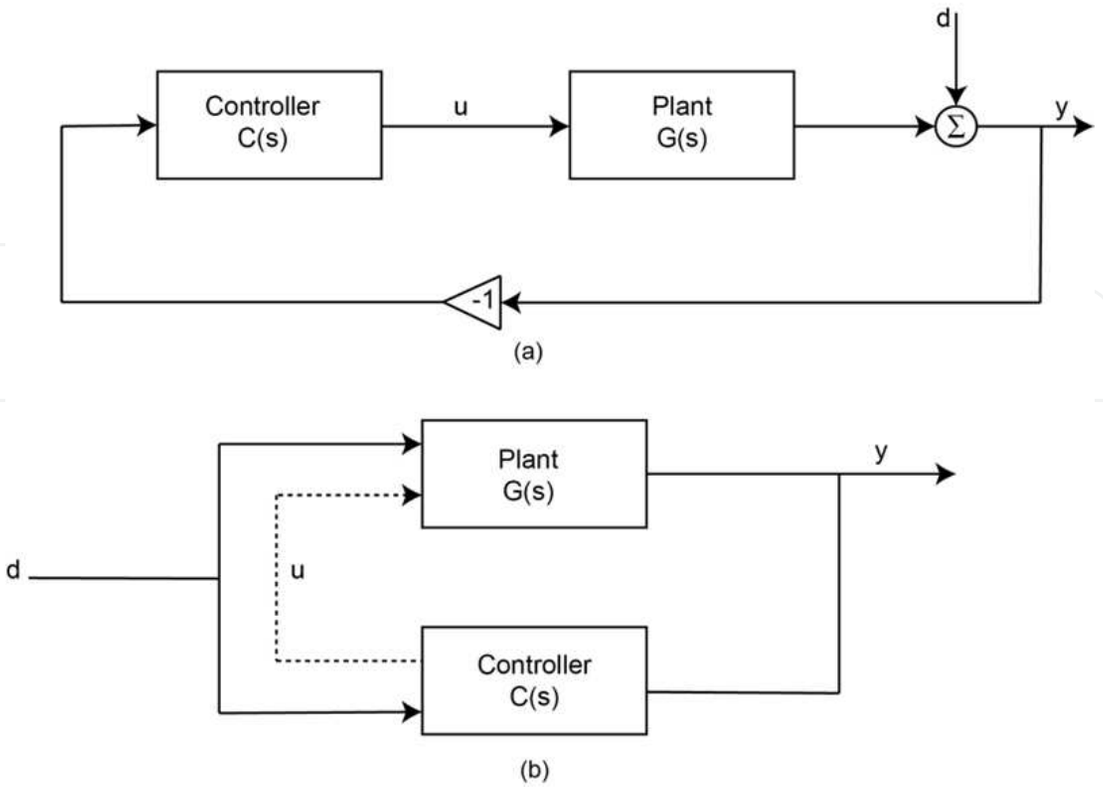

Figure 2. a) Feedback control block diagram b) Feedforward control block diagram

In the case of model-based controller, the open-loop system dynamics is represented with the state-space model as in Equation 3:

$$\begin{aligned} \dot{\mathbf{x}} &= \mathbf{A}\mathbf{x} + \mathbf{B}\mathbf{u} + \mathbf{B}_\mathbf{d}\mathbf{d} \quad \text{(a)} \\ \mathbf{y} &= \mathbf{C}\mathbf{x} + \mathbf{D}\mathbf{y} \quad \text{(b)} \end{aligned} \tag{3}$$

In this state-space form, **x** is the state variable**,** **y** is the measured output, **u** is the input signal and **d** is the external disturbance signal. In addition to these, **A** presents the state matrix, **B** is the controller input matrix**,** $\mathbf{B_d}$ is the disturbance matrix, **C** is the output matrix and **D** is the feed-through matrix. For full-state feedback controller ($u = -\mathbf{K}x$), the closed-loop system can be obtained as

$$\begin{aligned} \dot{x} &= (\mathbf{A} - \mathbf{B}\mathbf{K})\mathbf{x} + \mathbf{B}_\mathbf{d}\mathbf{d} \quad \text{(a)} \\ \mathbf{y} &= (\mathbf{C} + \mathbf{D}\mathbf{K})\mathbf{x} \quad \text{(b)} \end{aligned} \tag{4}$$

The aim of this state-space closed-loop system is to eliminate the effect of disturbance on output signal similar to the active damping. The gain matrix **K** can be determined by applying pole-placement or optimal control design methodologies.

2.3. Design of controller architecture

For control applications, it is necessary to understand the system dynamics appropriately since the controller design parameters are determined based on the system dynamics. As

stated in section 2.2 there are different types of the control algorithms and for each type of the controller, system identification is essential. This system identification can be carried out via a vibration testing & analysis methods. Aim of such method is to extract Frequency Response Functions (FRF) where these functions presents the system response to a specific input in frequency range of interest by means of magnitude and phase. A representative FRF is shown in Fig. 3 for a structure where piezoelectric materials are used as bonded patch actuators (to excite the structure) and LDV as velocity sensor (to measure the vibration response) .

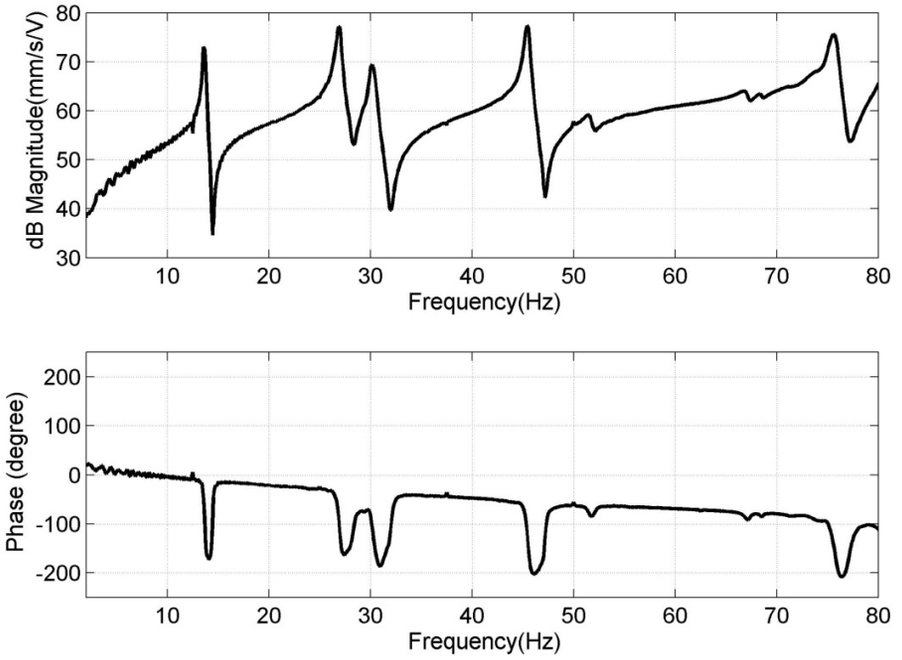

Figure 3. Example FRF of a system

The modal (resonance) frequencies of the systems are indicated in magnitude plot of FRFs as sharp peaks where the active damping systems are most effective. In active damping systems, the higher frequency modes may deteriorate the stability due to phase lag. Such effects of the higher frequency modes can be suppressed by including the low-pass filters. On the other hand, model based controllers use mathematical relations which in turn represents the system response based on FRF. Since the scope of this chapter is devoted only to proportional analog velocity feedback controller, more detailed information on model-based controllers and mathematical system representations can be found in references [6, 7, 9, and 12].

3. Application of analog velocity feedback controller

In this section an active vibration control system using an analog velocity feedback algorithm is described. At first, the system architecture is explained. Later, the controller design and implementation steps are discussed. In the final step, the evaluation of the controller performance is presented.

3.1. System architecture

The structure used in this study is a rectangular box (1 x 1 x 2 m) and shown in Fig. 4. The surrounding cavity walls are constructed using wood filled concrete with a thickness of 10 mm. This box is separated inside with a thin plate to obtain two enclosed compartments. The two compartments are used for investigation of vibration and noise transmission. The thin steel separation plate (1 x 1 m) in the rectangular box has a thickness 1.8 mm and clamped along on all four edges.

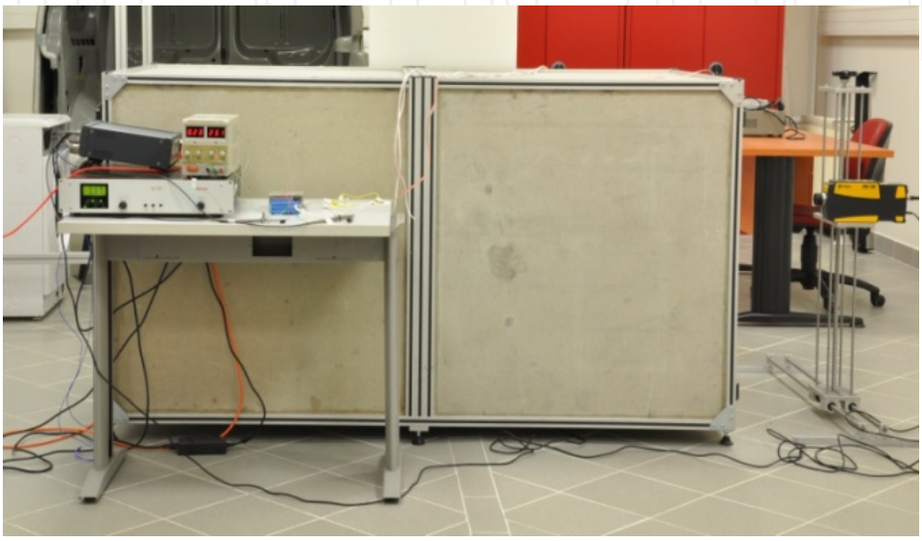

Figure 4. Rectangular box for vibration and noise reduction experiments

In the presence of mechanical and acoustical vibrations, the thin separation plate transmits the vibration and noise to the compartments. By attenuating vibrations of the separation plate, the noise radiation can be also reduced. In this study, the piezoelectric patch actuators bonded on the separation plate are employed as actuators to control and suppress vibration. The piezoelectric actuator is a PI Dura-act 875 bender type piezoelectric patch. This type of patch is compact, lightweight and insulated so it can be easily attached to the host structure and it does not add additional weight. The mechanical properties of the steel and piezoelectric patches are given in Table 1.

Since the piezoelectric materials generate high strain on the host structure, the most effective position for the piezoelectric patch is around the high strain regions on the host structure. In fact, for a clamped-clamped plate, the maximum curvature (highest strain region) changes over the surface for each vibration mode. The maximum curvature of the first mode of a clamped-clamped plate occurs at the center and along the edges; whereas in the second vibration mode, maximum curvature is in the middle of the upper and lower halves of the plate. After these high strain regions are identified, the piezoelectric patches are attached to the center and upper-left (-35 cm, 35 cm from the left upper corner) of the plate in order to suppress first two modes. For suppression of vibration and noise, two piezoelectric patches are used in independent and pair configuration. Fig. 5 shows the thin-separation plate and piezoelectric patches.

Property	Steel	Piezoelectric Patch
Length (mm)	1000	65
Width (mm)	1000	31
Depth (mm)	1.5	0.5
Elastic modulus (GPA)	190	70.2
Poisson's ratio	0.33	0.36
Density (kg/m3)	6305	7800
Piezoelectric Strain Constant d_{31} (10^{-10} m/V)	-	1.74
Piezoelectric Strain Constant d_{33} (10^{-10} m/V)	-	3.94
Piezoelectric Strain Constant d_{51} (10^{-10} m/V)	-	5.35

Table 1. Mechanical properties of host structure and piezoelectric patch

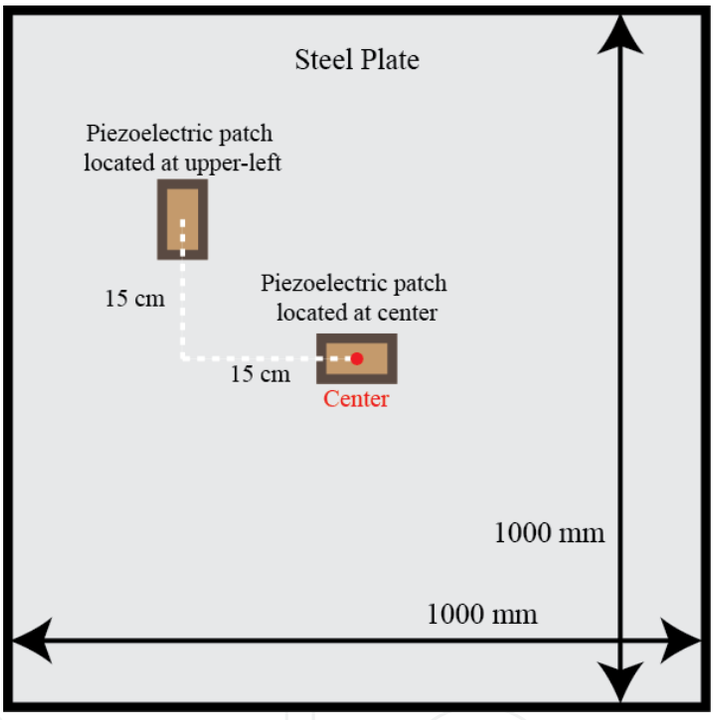

Figure 5. Thin steel plate with piezoelectric patches

3.2. Controller architecture

This section presents design and implementation of the active vibration controller via piezoelectric actuators. At first, proportional feedback controller is presented and then analog implementation of the controller is explained.

3.2.1. Design of proportional feedback controller

Proportional feedback control is a very simple and easily implementable controller methodology. Since only a sensor signal is passed through a negative amplifier and fed back to the system, the total computational and implementation cost is very low. Thus, it is possible to apply this control scheme using analog circuits since it does not need online

calculation of parameters such as controller gains and current states' values. In addition to these, by using collocated sensor and actuator pair, proportional feedback controller provides active damping at the resonance frequencies of the structure. In fact, this active damping can be employed effectively in the lower-frequency modes of the structure because of stability issues. At the high-frequencies, the phase lag may deteriorate the stability of the collocation and the closed-loop system can be unstable. This high-frequency stability problem is eliminated usually by decreasing the proportional gain or including a low-pass filter in the closed-loop. In this paper, we consider a proportional velocity feedback controller along with a low-pass filter to eliminate high-frequency dynamics.

The undesired vibrations of the thin separation plate are originated by external disturbances and the controller is designed for the expected disturbances including frequencies up to the third resonance mode. By only aiming low-frequency vibration suppression of the plate, high frequency performance of the controller is not considered. For this purpose, a low pass filter which has a cut-off frequency around third resonance mode is considered. In order to have decay at the frequencies higher than the cut-off frequency, the filter is included as an input low-pass filter and is placed between the sensor signal and the controller.

Then, the amplifier gain is adjusted by utilizing the tools of Ziegler-Nichols method. In Ziegler-Nichols method, the important step is the determination of critical gain (gain margin of the closed-loop system). This critical gain is defined as the amplifier ratio at which response of the controlled plant has sustained oscillations and closed-loop system is at the stability limit. Proportional feedback criterion of Ziegler-Nichols method claims that 0.8 times the critical gain yields the best proportional controller performance.

Having determined the cut-off frequency of the filter and amplifier ratio, the proportional velocity feedback controller is finalized for the implementation and experiments.

3.2.2. Implementation of velocity feedback controller

The designed proportional velocity feedback controller is implemented on a breadboard by using the circuit shown in Fig. 6. This analog circuit includes one inverting amplifier and low-pass filter.

The measured sensor voltage signal (V_{in}) is passed through a low pass filter which is in the form of resistor-capacitor (RC) filter. The cut-off frequency of this filter equals to one divided by multiplication of resistor and capacitance value. The aim of this low-pass filter is the reduction of high-frequency components of the sensor signal. After passing through this filter, the filtered signal is fed to the inverting amplifier. This inverting amplifier includes an operational amplifier (op-amp) and two resistors as indicated in Fig. 6. The op-amp is powered by dual polarity. The filtered sensor voltage is connected through input resistor R_c to the positive input channel of the op-amp. Then, a jumper resistor R_f is included between positive input channel and the output channel, whereas negative input channel is connected to the ground. By passing through this inverting amplifier, the sign of filtered sensor signal is inverted and its voltage value is amplified. The amplifier ratio is equivalent the ratio of jumper resistor R_f and input resistor R_c. Finally, this amplified and inverted signal serves as the proportional controller output signal.

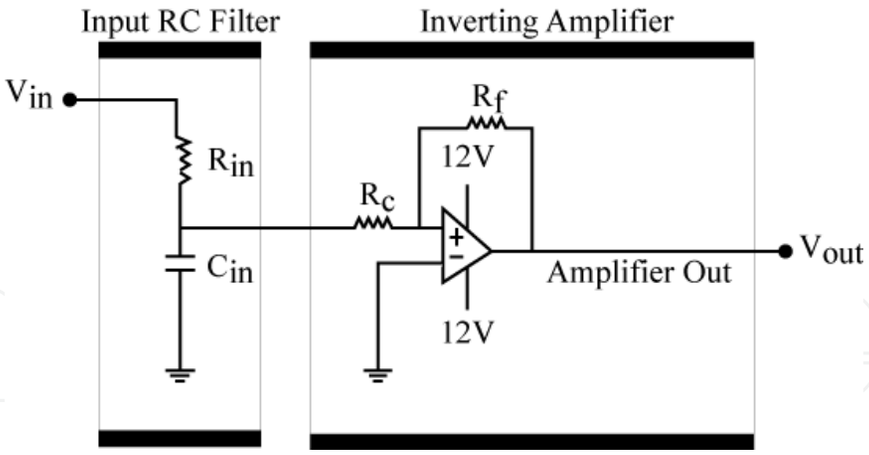

Figure 6. Implementation diagram for analog proportional velocity feedback controller

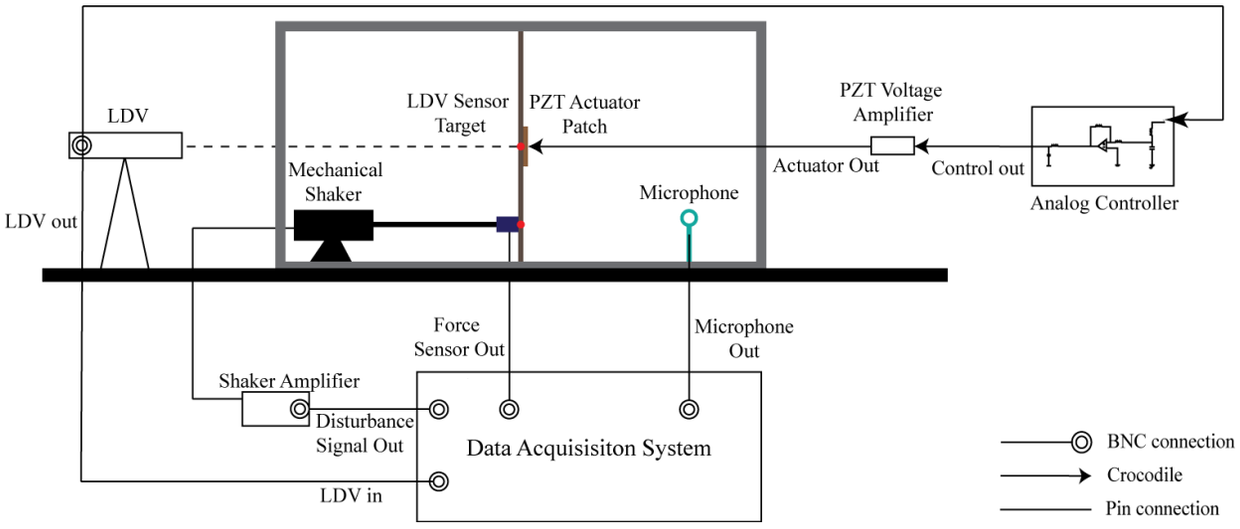

Figure 7. Experimental setup for active vibration and noise reduction

3.3. Experimental setup

The experimental setup for active vibration control via analog velocity feedback controller is presented in Fig. 7 with the data acquisition system. The data acquisition system has the ability of generation and recording analog voltage signal while communicating with a PC through Ethernet connection. The system provides high frequency sampling with high measurement accuracy and also generates the disturbance signal to drive the shaker amplifier. The mechanical shaker is located in the left compartment in Fig.4, and attached to the thin-separation plate via a connecting rod and a force sensor. The vibration of this plate is measured by Polytech PDV100 laser Doppler vibrometer (LDV). The target location of the vibrometer is determined as the same point of the piezoelectric patch to obtain a collocated sensor and actuator pair. The voltage output of the LDV is connected to the analog controller as a sensor signal and sent to the data acquisition system for recording. By connecting the sensor signal to the analog circuit, the controller output signal is acquired. This controller signal is amplified by E-413 Dura-act Piezo Driver and sent to the PZT patches (Dura-act P876.A12). Control input voltage between -2V and +8V are accepted by

the voltage amplifier and the input signal is amplified by factor of 50. By closing-the-controller loop, an active damping system for vibration suppression is created. While the vibration suppression experiments are conducted, the output signal of a microphone properly located in one of the compartments is also recorded at the same time to demonstrate the suppression of noise.

3.4. Results

In this section, active vibration suppression of the thin separation plate and noise reduction inside the compartment via analog velocity feedback controller is presented. The experimental results are given in frequency and time domains for three different piezoelectric patch configurations. At first, the piezoelectric patch located at center and upper-left is used as an actuator independently, and then they are employed together as an actuator.

3.4.1. Suppression of vibration in time domain

The performance of the analog velocity feedback control for the vibration suppression is evaluated in the time domain by disturbing the thin separation plate with the mechanical shaker. For this purpose, disturbance signal is applied to the mechanical shaker via data acquisition unit as a sine-wave at the first resonance frequency (approximately 13 Hz) and at the second-resonance frequency (approximately 26 Hz) of the plate. The vibration of the plate is monitored by targeting laser displacement to the center of the piezoelectric actuator patch. The experiments are conducted for each piezoelectric actuator configuration. Fig. 8 presents the results for forced vibration at the first resonance frequency. Fig. 8 (a) presents the open-loop vibration at the center of the plate. The open-loop response corresponds to the structural vibrations of the thin plate when the analog feedback controller is inactive. Fig. 8(b) shows the closed-loop vibration response of the plate when the active vibration suppression is obtained via piezoelectric patch located at center. In Fig. 8(c), the piezoelectric patch located at upper-left and is employed as actuator independently. The Fig. 8(d) shows the closed-response for the piezoelectric actuator in pair configuration where the center and upper-left patch are used as actuator jointly and laser displacement sensor is targeted to the center of the upper-left patch.

As can be seen from the subfigures of Fig. 8, the vibration of the plate at the first resonance frequency is attenuated for each piezoelectric actuator configuration. In fact, the best performance is acquired when the piezoelectric center patch is used as actuator independently. The performance of this configuration is better than the pair configuration because of phase mismatch of the piezoelectric patches in pair. Fig. 8 presents the open and closed vibration of the plate for the second resonance forced vibration. To measure the open-loop vibrations of the plate, the LDV is targeted to the center of the upper-left patch. Fig. 9(a) presents the open-loop vibration measured at this location. Fig. 9(b) shows the performance of the active vibration control via piezoelectric actuator patch located at the upper-left of the plate. Besides, Fig. 9(c) presents the effectiveness of piezoelectric pair configuration for the vibration suppression of the plate.

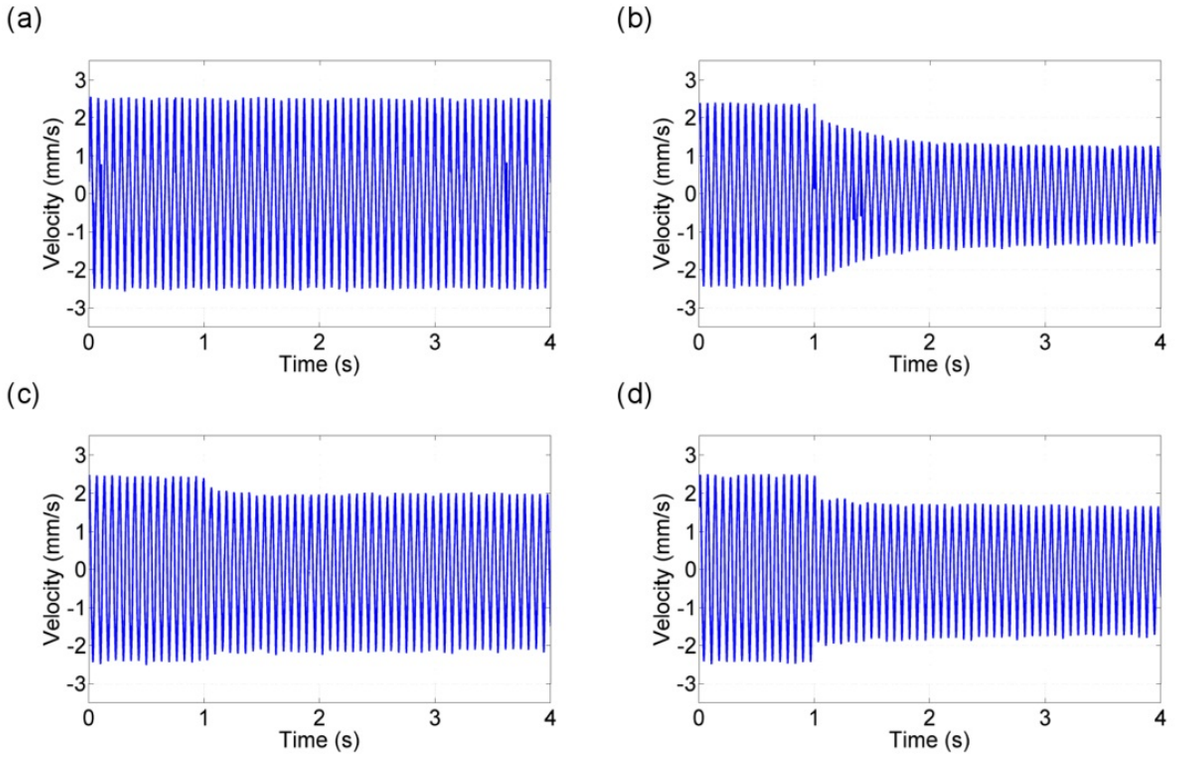

Figure 8. Vibration response of the plate at the first resonance frequency (a) Open-loop (b) Closed-loop with piezoelectric patch located at center (c) Closed-loop with piezoelectric patch located at upper-left (d) Closed-loop with piezoelectric actuator patches in pair

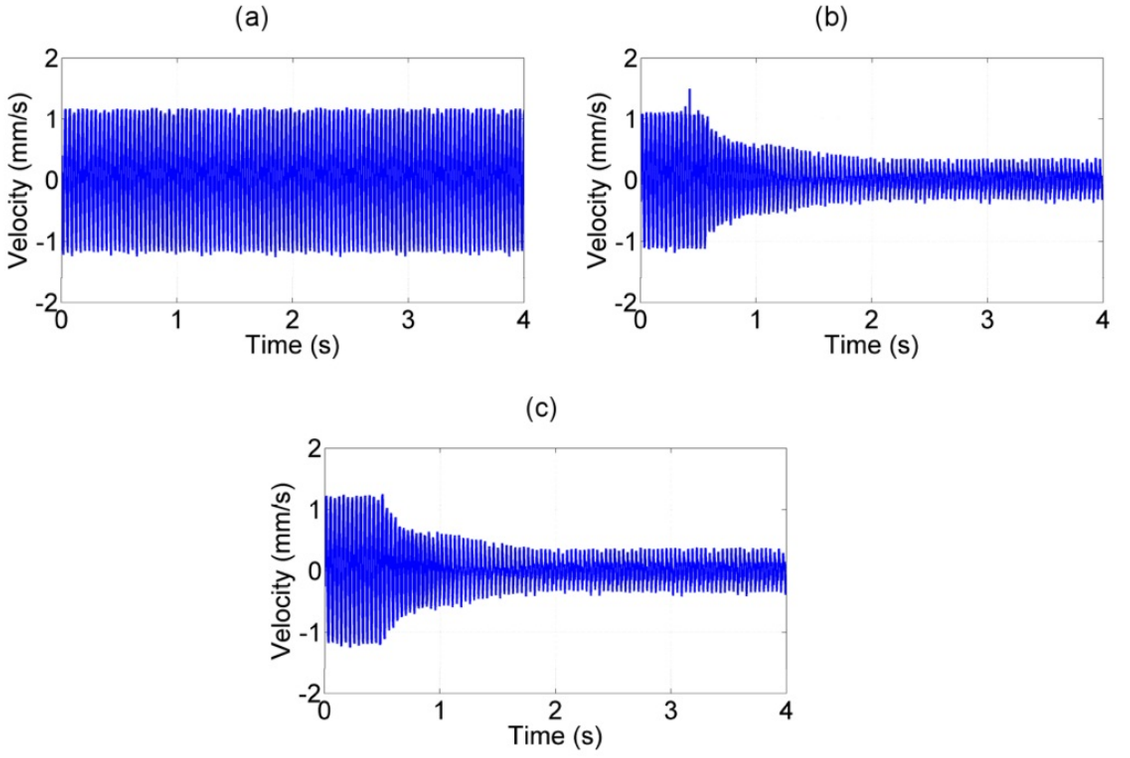

Figure 9. Vibration response of the plate at the second resonance frequency (a) Open-loop (b) Closed-loop with piezoelectric patch located at upper-left (c) Closed-loop with piezoelectric actuator patches in pair

Piezoelectric Patch Configuration	LDV Target Location	First Mode	Second Mode
Center	Center	44.6% (5.1dB)	-
Upper-left	Center	20.4% (1.9 dB)	73.8% (11.6 dB)
Center and Upper-left (Pair Configuration)	Upper-left	32.3% (3.4 dB)	74.9% (11.9 dB)

Table 2. Vibration suppression levels in time domain for different piezoelectric actuator configurations

To employ piezoelectric patches in pair for the second resonance mode of the plate, the LDV is targeted again to the center of the upper-left piezoelectric patch. It is obvious that the independent configuration of piezoelectric patch located at upper-left provides better vibration suppression when it is compared with the pair configuration. The reduction levels for each configuration are presented in Table 2.

3.4.2. Supression of vibration in frequency domain

The aim of this section is to present the performance of the active vibration suppression in the frequency domain. The experiments are conducted for the same piezoelectric actuator configurations. In contrast to time-domain results, the disturbance signal applied to the mechanical shaker is changed to sine-sweep in the bandwidth of 2 Hz to 100 Hz. By monitoring the open-loop and closed-loop response of the plate, frequency responses are gathered using the data acquisition system. Fig. 10 presents the frequency responses for different piezoelectric configurations between vibrometer and the force transducer at the tip of the mechanical shaker. In Fig. 10(a), the performance of the active vibration suppression system via piezoelectric patch located at center is presented. It is noticeable that the vibration is attenuated very well in the first resonance mode of the plate; however the other resonance frequencies of the plate are not affected. This is due to the fact that the position of piezoelectric patch located at center corresponds to the anti-mode of the higher order modes. So, the higher structural modes are not affected. Fig. 10(b) presents the closed-loop performance of the piezoelectric patch located at upper-left. As can be seen this figure, the closed-loop system reduces the vibration of the plate in a broad frequency range for this configuration. Fig. 10(c) shows the effectiveness of the closed-loop system via piezoelectric actuator pair. It is noticeable that the performance of the closed-loop is improved considerably when piezoelectric pair configuration is adopted instead of using upper-left patch independently. Indeed, the closed-loop system reduces the vibration levels as compared to open-loop in all piezoelectric actuator configurations. Table 3 lists the vibration reduction levels in the frequency domain.

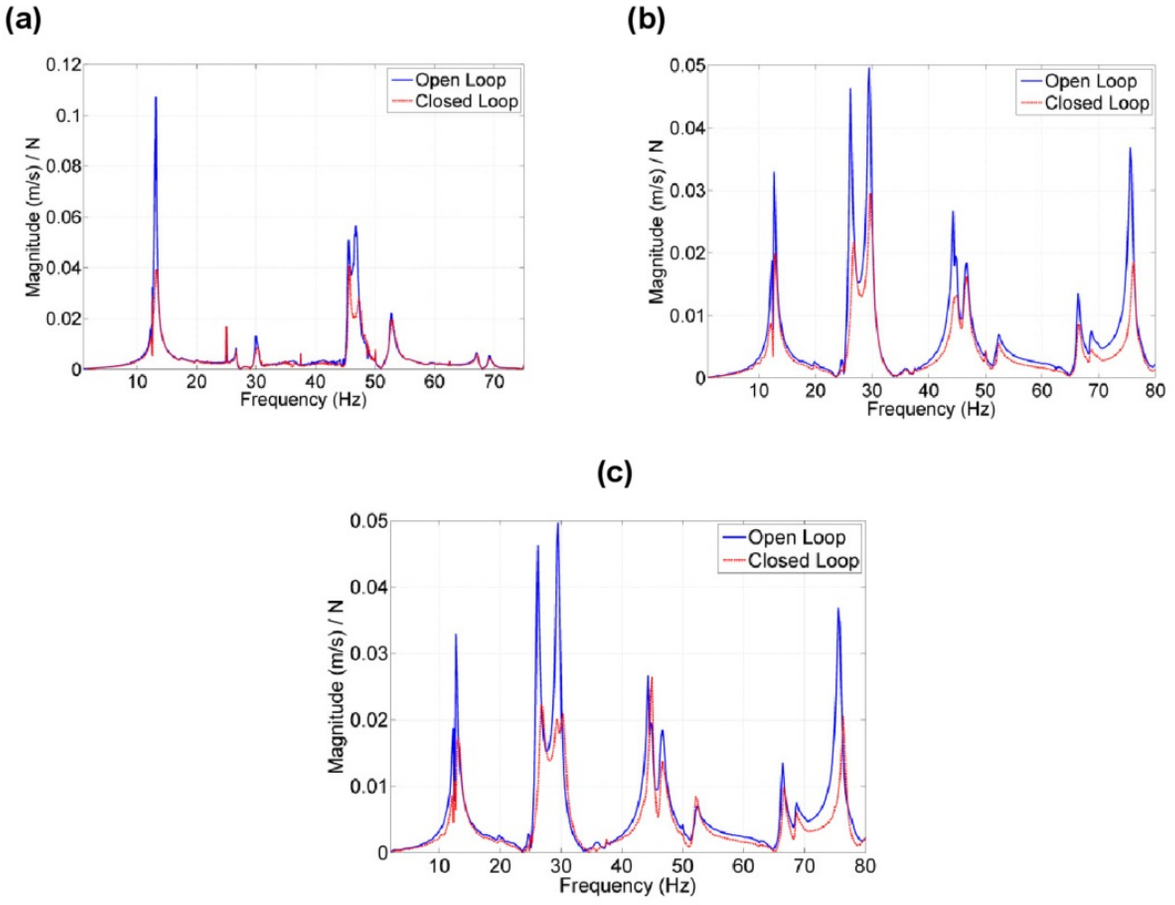

Figure 10. Frequency responses for different piezoelectric actuator configurations (a) Closed-loop with piezoelectric patch located at center(LDV at center) (b) Closed-loop with piezoelectric patch located at upper-left(LDV at upper-left) (c) Closed-loop with piezoelectric actuator patches in pair(LDV at upper-left)

Piezoelectric Patch Configuration	LDV Target Location	First Mode	Second Mode
Center	Center	63.7 % (8.8 dB)	-
Upper-left	Center	34.1 % (4.4 dB)	52.8 % (6.5 dB)
Center and Upper-left (Pair Configuration)	Upper-left	50.6 % (6.1 dB)	54.0 % (6.7 dB)

Table 3. Vibration suppression levels in time domain for different piezoelectric actuator configurations

3.4.3. Suppression of noise in frequency domain

This section presents the noise reduction in one of the compartments for controller-inactive and active cases while disturbing the thin plate via shaker. The noise inside the compartment is measured with a microphone. The frequency responses between the microphone and the force transducer are gathered using the data acquisition system. Fig. 11

presents the results for noise in the frequency domain. As in the same manner with vibration suppression experiments, open-loop response shows the noise radiation in the compartment when the controller is inactive, whereas closed-loop response is monitored when the controller is active. In Fig. 11(a), the performance of noise reduction via piezoelectric patch located at center is given. It is noticeable that the low-frequency acoustic mode in the compartment coincides with the vibration mode of the plate. Since the vibration of plate at the first resonance mode is considerably attenuated, the noise radiation is also reduced for this mode. At the higher-acoustics modes, the closed-loop system does not improve and deteriorate the noise radiation in the compartment. Fig. 11(b) presents the effectiveness of the piezoelectric patch located at upper-left. Similar to the previous results, noise radiation is reduced by suppressing the vibration of the plate. However, it is obvious that the performance of the piezoelectric patch located at center is fairly better than the performance of the piezoelectric patch located at upper-left.

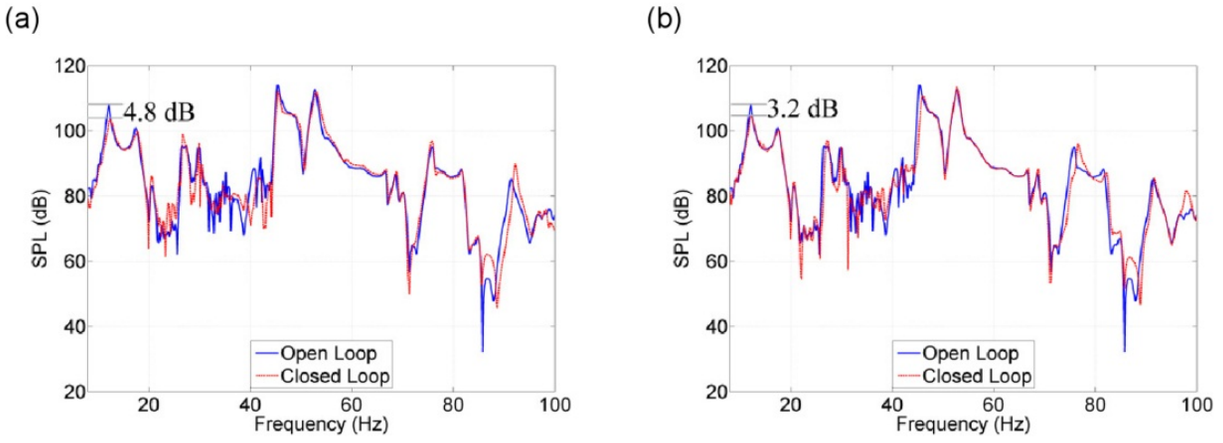

Figure 11. Noise levels in the one of the compartments for different piezoelectric patch configurations (a) Open and closed-response for the piezoelectric patch located at center (b) Open and closed-loop response for the piezoelectric patch located at upper-left

4. Conclusion

In the first part of this chapter, a short review of literature about active vibration control is presented. The general controller design approach and the differences between various controller algorithms are discussed.

In the second part of this chapter, an application using an analog velocity feedback controller for vibration suppression of a flexible plate is presented. Experiments for vibration suppression of the flexible plate are conducted and by measured the vibration of the plate; the time-responses and frequency-responses are presented. Finally, the acoustic response in one of the compartments is also obtained for different piezoelectric actuator configurations. The results revealed that vibration reduction of the separation plate improves the noise radiation and the sound pressure level is decreased due to the reduction of the vibration. However, for an effective and powerful noise reduction, robust controller algorithms with multiple piezoelectric actuator patches can be preferred.

Author details

Ipek Basdogan*, Utku Boz, Serkan Kulah and Mustafa Ugur Aridogan
Koç University, Turkey

5. References

[1] Bailey T, Hubbard J.E. Distributed Piezoelectric Polymer Active Vibration Control of a Cantilever Beam. Journal of Guidance Control and Dynamics 1985;8(5): 605-611.
[2] Crawley E.F, De Luis J. Use of Piezoelectric Actuators as Elements of Intelligent Structures. AIAA Journal 1987; 25: () 1373-1385.
[3] Ro J, Baz A, Control of Sound Radiation from a Plate into an Acoustic Cavity Using Active Constrained Layer Damping. Smart Materials and Structures 1999; 8(3): () 292.
[4] Rao S.S, Sunar M. Piezoelectricity and Its Use in Disturbance Sensing and Control of Flexible Structures: A Survey. Applied Mechanics Reviews 1994; 47(4):113-123.
[5] Loewy R.G, Recent Developments in Smart Structures with Aeronautical Applications. Smart Materials and Structures 1997; 6(5): R11.
[6] Chee C.Y.K, Tong L, Steven G.P. A Review on the Modelling of Piezoelectric Sensors and Actuators Incorporated in Intelligent Structures. Journal of Intelligent Material Systems and Structures 1998; 9(1): 3-19.
[7] Alkhatib R, Golnaraghi M.F. Active Structural Vibration control: A review, Shock and Vibration Digest 2003; 35(5):367-383.
[8] Gupta V, Sharma M, Thakur N. Optimization Criteria for Optimal Placement of Piezoelectric Sensors and Actuators on a Smart Structure: A Technical Review. Journal of Intelligent Material Systems and Structures 2010; 21(12):1227-1243.
[9] Iorga L, Baruh H, Ursu I. A Review of H_∞ Robust Control of Piezoelectric Smart Structures. Applied Mechanics Reviews 2008; 61(4): 040802-040815.
[10] Chopra I. Review of State of Art of Smart Structures and Integrated Systems. AIAA Journal 2002; 40(11):2145-2187.
[11] Hanselka H. Adaptronics as a Key Technology for Intelligent Lightweight Structures. Advanced Engineering Materials 2001;, 3: 205-215.
[12] Preumont A. Vibration Control of Active Structures : An Introduction, 2 ed. Kluwer Academic: New York; 2002.
[13] Hurlebaus S, Gaul L. Smart Structure Dynamics. Mechanical Systems and Signal Processing 2006; 20(2):255-281.

* Corresponding Author